# Single chain spectroscopy of conformational dependence of conjugated polymer photophysics

**Thomas Huser*†, Ming Yan*, and Lewis J. Rothberg‡**

*Department of Chemistry and Materials Science, Lawrence Livermore National Laboratory, M/S L-250, Livermore, CA 94551; and ‡Department of Chemistry and Center for Photoinduced Charge Transfer, University of Rochester, Rochester, NY 14627

Communicated by Esther M. Conwell, University of Rochester, Rochester, NY, August 15, 2000 (received for review June 30, 2000)

**Single molecule confocal fluorescence microscopy was used to perform photoluminescence spectroscopy on single, isolated molecules of the conjugated polymer poly[2-methoxy,5-(2′-ethylhexyloxy)-*p*-phenylene-vinylene] (MEH-PPV). We show that the fluorescence from single chains of this electroluminescent polymer depends strongly on chain conformation. The time evolution of the spectra, emission intensity, and polarization all provide direct evidence that memory of the chain conformation in solution is retained after solvent evaporation. Chains cast from toluene solution are highly folded and show memory of the excitation polarization. Exciton funneling to highly aggregated low energy regions causes the chain to mimic the photophysical behavior of a single chromophore. Chains cast from chloroform, however, behave as multichromophore systems, and no sudden discrete spectral or intensity jumps are observed. These also exhibit different spectroscopy from the folded chromophores.**

Recent advances in instrumentation have allowed the detection and manipulation of single molecules at room temperature (for recent reviews see, e.g., ref. 1). These techniques have led to the observation of physical effects and properties of individual molecules that could not be probed by previous ensemble-averaging studies. For example, measurements of inter- and intramolecular binding forces and elastic moduli of biological macromolecules by magnetic beads (2, 3), atomic force microscopy (4), hydrodynamic flow (5), or optical tweezers (6) have provided significant insight to the mechanical properties of DNA and proteins. Single molecule fluorescence detection has seen particular interest, because the fluorescence labeling of DNA, RNA, enzymes, and proteins allows for dynamic studies of macromolecular interactions and function, such as complexation (7). The optical visualization of these molecules, however, requires specific labeling with fluorescent dyes or the use of intercalating dyes.

Single molecule studies of intrinsically fluorescent macromolecules, such as photosynthetic light harvesting complexes (8) or the green fluorescent protein (9), have exhibited interesting quantum effects. Protein molecules with several chromophores, for example, were shown to behave as a single quantum system (10). The close packing of chromophores in such proteins leads to strong interchromophore interaction that gives rise to cooperative effects such as intermittent fluorescence (11, 12) and photon-antibunching (10). Single molecule fluorescence studies of green fluorescent protein revealed similar intermittent fluorescence (9).

Most remarkably, intermittent fluorescence together with the observation of discrete emission levels was also reported for single molecules of conjugated polymers estimated to consist of over 1000 chromophores (13). Another surprising result is the recent observation of efficient photoluminescence quenching of polymer chains by extremely low amounts of cationic electron acceptors (14), which provides a unique bio-probe scheme with high multiplication yield. However, these results raise some fundamental questions about interchromophore interactions in conjugated polymers. What mechanism causes these polymers to behave like a single quantum system, and can this be avoided in systems where stable fluorescence is desirable?

Conjugated polymers, such as poly[2-methoxy,5-(2′-ethylhexyloxy)-*p*-phenylene-vinylene] (MEH-PPV), are synthetic molecules with a backbone of conjugated carbon double bonds. Kinks, bends, or chemical defects break the conjugation of the backbone in individual segments, thus resulting in a chain of linked chromophores. This allows these materials to transport charge and to luminesce efficiently (15). Their solubility is determined by the side groups attached to the backbone. Side groups that facilitate good solubility of conjugated polymers in common solvents allow for easy processing and inexpensive mass production of electronic thin film devices. Because of their size and relative flexibility, however, polymer molecules are able to aggregate to lower their energy. Conjugated polymer film studies show that aggregation leads to the formation of weakly emissive interchain species in thin films that significantly reduce the quantum yield of thin film devices (16). The formation yield of interchain species remains a subject of study (17), but there is emerging a consensus that the strong processing dependence of luminescence yields results from film morphology (18, 19). Indeed, the conformation of chains in films has been shown to be correlated to the molecular conformation in solution (18).

Here, we show that fluorescence from single chains of the conjugated polymer MEH-PPV spun-cast onto an inert surface depends strongly on chain conformation.

Highly folded chains show memory of the excitation polarization. Very efficient three-dimensional exciton funneling to highly aggregated low energy regions causes these chains to act similar to a single chromophore. Extended chains, on the other hand, behave as multichromophore systems with little interaction between individual segments. These results show an astounding similarity to effects observed in single fluorescent proteins and suggest a potential connection between the properties of biological and synthetic macromolecules.

## Results and Discussion

We obtained diffraction-limited photoluminescence images of individual chains of MEH-PPV with a modified upright confocal fluorescence microscope similar to recent reports (20) (see Fig. 1 *a* and *c*). The molecular weight of the MEH-PPV used for this study was about 1,000,000 with a polydispersity of 7.6 as determined by gel permeation chromatography. Samples were prepared by first spin-casting a cover glass surface with a $10^{-9}$ to $10^{-10}$ M polymer solution and subsequent deposition of a 70-nm polyvinylbutyral (PVB) film to prevent fast photobleaching. Polymer solutions were prepared from two different solvents. MEH-PPV in the nonpolar solvent Toluene tends to form a tight coil to minimize solvent interactions, whereas, in the more polar solvent chloroform, the polymer chains are expected to have an

Abbreviation: MEH-PPV, poly[2-methoxy,5-(2′-ethyl-hexyloxy)-*p*-phenylene-vinylene].

†To whom reprint requests should be addressed. E-mail: huser1@llnl.gov.

The publication costs of this article were defrayed in part by page charge payment. This article must therefore be hereby marked "*advertisement*" in accordance with 18 U.S.C. §1734 solely to indicate this fact.

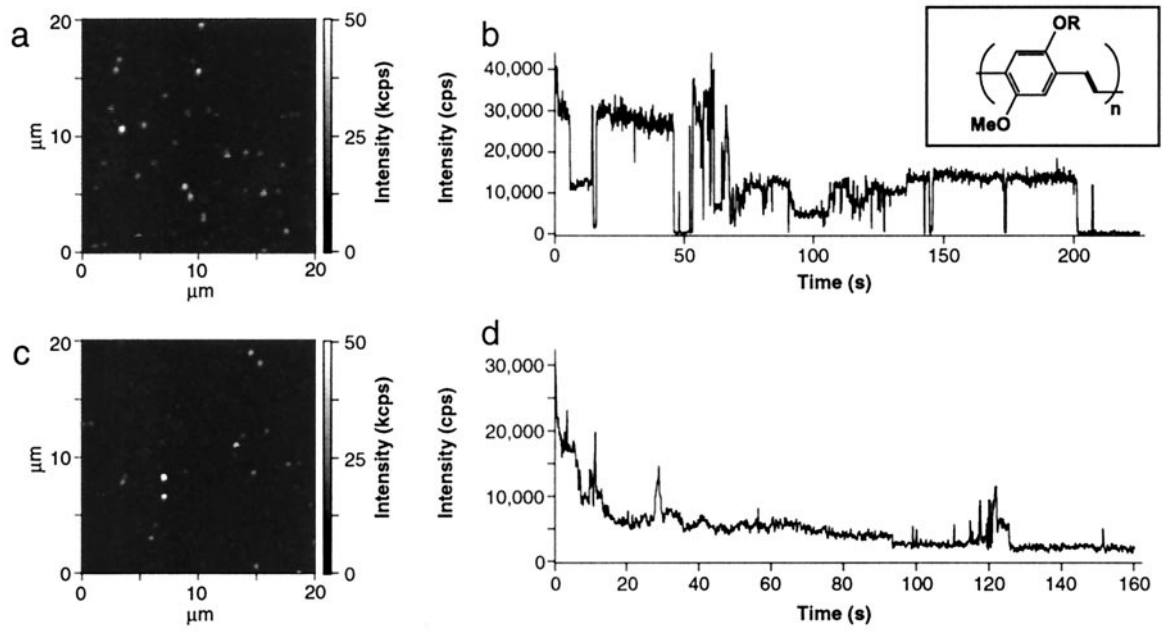


**Fig. 1.** Photoluminescence images and sample intensity transients for MEH-PPV/Tol (*a* and *b*) and MEH-PPV/Clf (*c* and *d*). Photoluminescence of the molecules was excited with 200 W/cm$^2$ at a wavelength of 488 nm and circular polarization. The intensity variation between the molecules may be because of the large polydispersity of the molecular weight. The *Inset* above *b* shows the chemical structure of MEH-PPV.

extended conformation (18). For the different samples, PVB cap layers were spin-cast from the same solvents, respectively.

The diffraction-limited spots observed in the single molecule images were attributed to single polymer molecules because the number of spots varies linearly with the concentration. Moreover, the number of spots on the surface equals roughly the density of molecules that is expected for the given concentration of the solution. Additional evidence comes from molecules spin-cast from toluene solution (MEH-PPV/Tol), where discrete photobleaching steps are observed and the emitters behave as if they have fixed absorption and emission dipole moments. These latter observations do not hold for molecules spin-cast from chloroform solution (MEH-PPV/Clf) for reasons that will become clear during the discussion of our results.

We have examined more than 100 molecules spun from each solvent. The photophysical behavior we observed for all of these molecules was similar. The data-acquisition procedure for these molecules was always kept the same: After taking an image at low power (70 W/cm$^2$), the spots were addressed by a circularly polarized excitation beam (488 nm) with a closed-loop piezo positioning stage (P-517.3CL; Physik Instrumente, Waldbronn, Germany). The excitation power was increased to 200 W/cm$^2$ and spectra with 5-s integration time and a spectral resolution of 1.5 nm were taken until the molecule underwent final photobleaching. Simultaneously, the overall emission intensity was monitored and split to two photodetectors at orthogonal polarization.

Fig. 1 shows photoluminescence images and representative intensity transients for molecules spin-cast from the two different solvents. Fig. 1*b* is an intensity transient for a MEH-PPV/Tol molecule. This molecule reveals intermittent fluorescence similar to that observed recently by VandenBout *et al.* (13). The photoluminescence intensity switches rapidly between on- and off-states while different, discrete intensity levels are assumed. This behavior has been explained by the creation of photogenerated defects that quench excitations along the entire chain (13). Fig. 1*d*, however, shows a very different behavior. The intensity transient for a MEH-PPV molecule spun cast from chloroform solution reveals an initial exponential decrease in its photoluminescence intensity without discrete jumps. This behavior is representative for all MEH-PPV/Clf molecules we measured. The time constants for the exponential intensity decrease vary from 0.1 to 2 s. After a few seconds, jumps in the intensity occur, but never to the background level. The further reduction of the intensity to the background level occurs gradually and on much longer time scales than that for MEH-PPV/Tol molecules.

To understand the physical origin of this very different behavior, we analyzed photoluminescence spectra obtained simultaneously with the intensity transients. Fig. 2 shows sample spectra vs. time for MEH-PPV/Tol and MEH-PPV/Clf molecules, respectively. MEH-PPV/Tol molecules (see Fig. 2 *a* and *b*) show well-resolved vibronic structure. The position of the first vibrational peak (0–0) typically lies at about 570 nm. The spectra shift by up to 50 nm to lower wavelengths under continued excitation, whereas the separation between the first and second vibrational peak remains constant with an energy spacing of 0.16 eV corresponding to the backbone stretching mode. Fig. 2*a* gives an example of this behavior where the initially red emission shifts to shorter wavelengths until the final photobleaching step occurs. Fig. 2*b* shows a very similar behavior with the spectrum at time 0 revealing a minor blue component that disappears after few seconds. In 75% of the 120 molecules we examined, we observe fully red-shifted spectra as shown in Fig. 2*a*. Only 25% of the spectra have an additional blue component.

Fig. 2 *c* and *d* show representative single molecule spectra of MEH-PPV/Clf molecules. The emission is relatively broad and without much vibronic structure. The peak emission typically lies at about 550 nm. The intensity (area under the spectra) decreases exponentially with the spectral mean fluctuating around an average value. Only 16% of the spectra show some initial vibronic structure superimposed on a broad background. This structure, however, is lost after a few seconds of exposure.

In a recent report, single molecules of MEH-PPV were shown to reveal a high degree of anisotropy of their absorption and emission dipole moments (21). We investigated this behavior further by separating the photoluminescence into two channels with orthogonal polarization. The ratio between these two

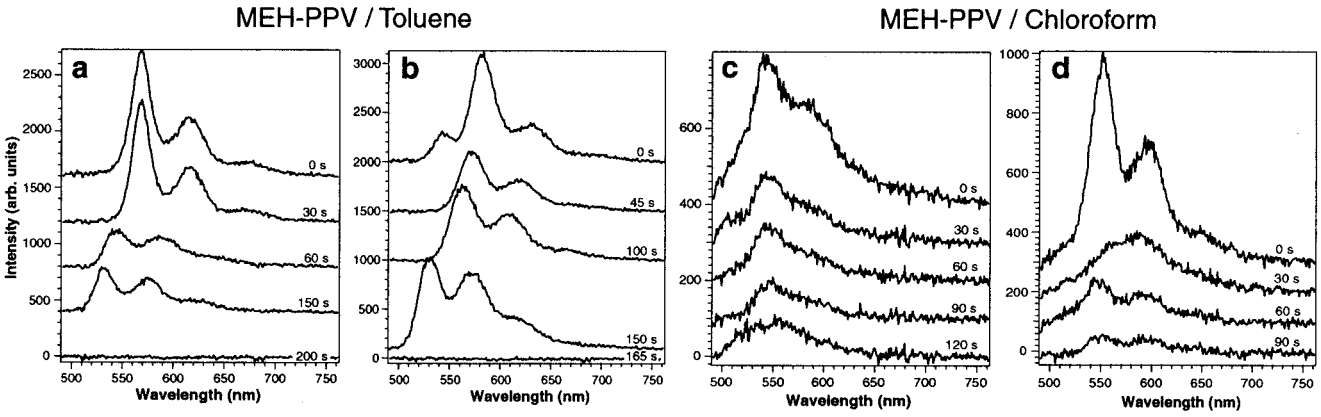


**Fig. 2.** Representative time-dependent spectra of MEH-PPV/Tol (*a* and *b*) molecules and MEH-PPV/Clf (*c* and *d*) molecules obtained under continuous excitation. Integration time for each spectrum was 5 s with a spectral resolution of 1.5 nm. Spectra are offset in vertical direction for clarity and labeled with the start time at which they were taken.

channels provides information on the orientation of the emission dipole moment relative to the excitation polarization. Fig. 3*a* shows a representative trace of the temporal evolution of spectral mean and polarization ratio for a single MEH-PPV/Tol molecule. The spectral mean has an initial value of 598 nm and stays at this value for the first 40 s. Then, it undergoes fluctuations with deviations from the former value of up to 15 nm, until it finally shifts to shorter wavelengths at about 140 s. The polarization ratio starts at 0.4 and shows short-term (<1 s) and long-term (several seconds) fluctuations that are related to the shifts in spectral mean. Fig. 3*b* shows the same representative comparison for a MEH-PPV/Clf molecule. Its spectral mean shifts slightly around an average value of about 576 nm. The polarization ratio starts at 0.1 and stays close to 0, indicating almost equal intensities for the two detectors.

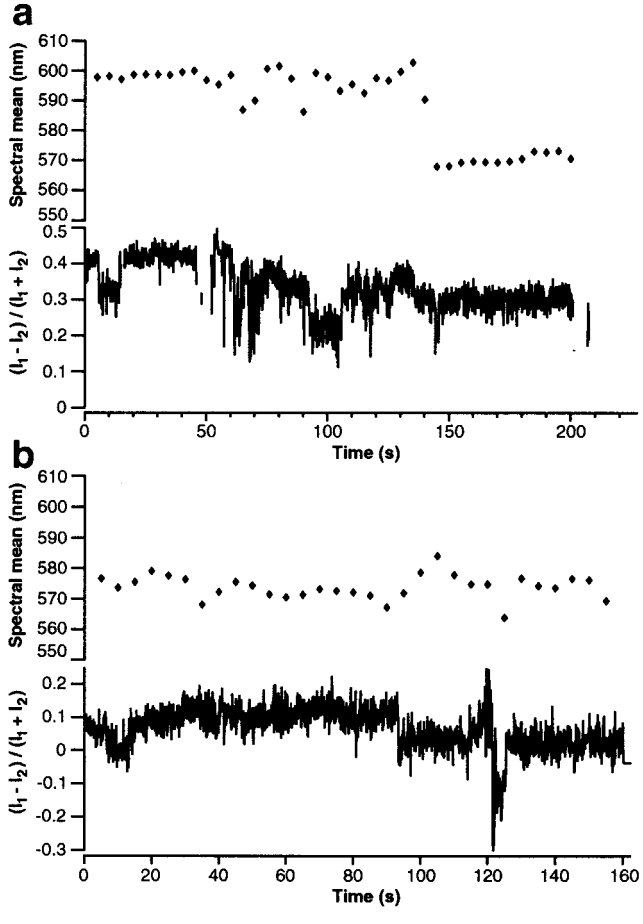


**Fig. 3.** Time evolution of spectral mean and polarization ratio $[(I_1 - I_2)/(I_1 + I_2)]$ for MEH-PPV/Tol (*a*) and MEH-PPV/Clf (*b*). MEH-PPV/Tol molecules show a polarization ratio distinct from 0, indicating a strong polarization anisotropy. Jumps to the background level were excluded and present themselves as gaps in the polarization ratio transient.

Histograms of the polarization ratios for 87 molecules spin-cast from toluene and chloroform, respectively, are shown in Fig. 4. These histograms were obtained from initial polarization ratios of molecules in image scans to prevent negative effects from previous exposure of such scans. The histogram for MEH-PPV/Tol molecules in Fig. 4*a* reveals high polarization anisotropy. The large distribution of polarization ratios indicates that MEH-PPV/Tol molecules have a well-defined emission dipole moment. The Gaussian distribution around an anisotropy value of 0 for MEH-PPV/Clf molecules in Fig. 4*b* indicates random emission (equal intensity at the two polarization sensitive detectors).

These observations are explained by a model of conformation-dependent intramolecular energy transfer if we assume that the MEH-PPV chains remember their solution configuration before deposition on the substrate. Polymer molecules in dilute toluene solution assume a tightly folded conformation, whereas those in chloroform take on a more extended conformation. This behavior has been verified for MEH-PPV by light-scattering experiments (18). A tightly coiled molecule allows for interactions between its closely stacked segments, thus facilitating efficient three-dimensional exciton diffusion (17). In addition, interchain stacking interactions appear to be responsible for reduction in luminescence yields and red-shifted spectra characteristic of longer conjugation in packed regions (16, 19, 22, 23).

In the case of MEH-PPV/Tol, the excitation energy is efficiently transferred to the longest segments. In the majority of cases (75%), the longest segments are the only emissive species. Only 25% of all molecules show partial energy transfer, as indicated by a weak emission from shorter segments. These presumably represent parts of the chain that are not tightly coiled and cannot transfer all their energy to the longer segments. Because energy transfer from the short conjugation segments to longer segments is very efficient and occurs within a few picoseconds (24), only the longest segments have a substantial occupancy of the excited states. Thus, only these will be attacked

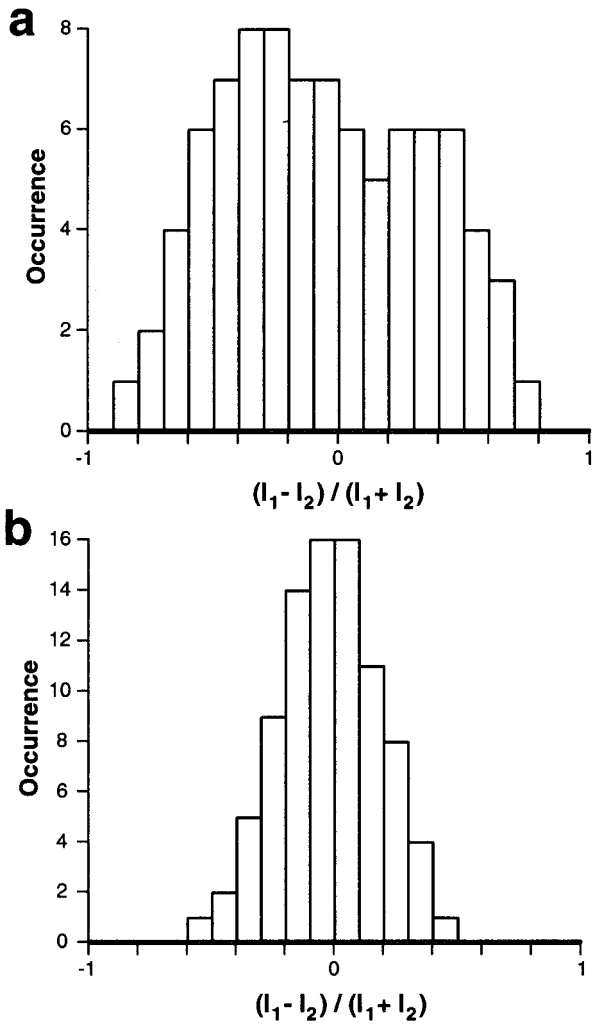


**Fig. 4.** Polarization ratio histograms of 87 molecules for MEH-PPV/Tol (*a*) and MEH-PPV/Clf (*b*), respectively.

by excited state photoreactions that create photochemical defects. Once all of the longer segments are photo-bleached, energy transfer to these segments is prohibited and the shorter segments become emissive as indicated by the blue-shifts in Fig. 2 *a* and *b*. The high polarization anisotropy for MEH-PPV/Tol as observed from the histogram in Fig. 4*a* indicates a fixed emission dipole moment. This can only be achieved for a polymer molecule with such high molecular weight by a well-organized folding of the polymer chain. Remarkably, the polarization memory is retained even after the longest segments are photodegraded, indicating that even the bluer emission that presumably comes from less aggregated regions with shorter conjugation lengths still derives from chain segments that are oriented with respect to the heavily aggregated regions.

A polarization anisotropy histogram for single dye molecules with fixed emission dipole moments would result in an even distribution of all anisotropy values. In the case of MEH-PPV/Tol molecules, we have never observed extreme values (1, −1), but the distribution is significantly broader than for MEH-PPV/Clf molecules. Such a result is expected for a self-aggregated polymer molecule with well-stacked segments. The high efficiency of intramolecular energy transfer for self-aggregated molecules explains intermittent fluorescence (13). All excitation energy is transferred to low energy regions. If those regions harbor a reversibly photogenerated quenching site such as charge separation on adjacent conjugation segments (polaron pair formation), the entire molecule's fluorescence can be temporarily quenched until charge recombination occurs. Similar processes are held responsible for the intermittent fluorescence of semiconductor nanocrystals (25). Efficient intramolecular energy transfer also explains the efficient photoluminescence quenching of polymer chains by extremely low amounts of cationic electron acceptors (14) and permanent loss of photoluminescence.

The spectroscopy of the initial emission in the toluene cast MEH-PPV (Fig. 2 *a* and *b*) is also informative. A higher intensity of the 0–0 peak with respect to the 0–1 peak is observed than is seen for the blue-shifted spectra that result after prolonged exposure or those in the chloroform case. The steric hindrance from packing makes the optical transition more vertical because the excited and ground states are driven toward having similar geometries. In addition, the suppression of the torsional motion results in an increase in effective conjugation length and hence redder emission spectra. Molecules spin-cast from chloroform, however, assume an extended conformation. In this case, energy migration along the chain becomes a more important pathway for energy transfer. Dipoles from segments along a chain are poorly situated for efficient Forster transfer and quasi-one-dimensional diffusion along the chain direction is slow (26). Therefore, the photoluminescence spectra of MEH-PPV molecules with extended conformation as shown in Fig. 2 *c* and *d* exhibit a broad emission from multiple emitting segments. The shape of the emission spectrum therefore results from a distribution of chromophores with a variety of conjugation lengths. Because energy transfer is inefficient, the emission of multiple segments with different conjugation lengths leads to nearly homogeneous photobleaching of all segments. Thus, the intensity transient in Fig. 1*d* shows an exponential decrease. The Gaussian distribution of the polarization anisotropy around 0 in Fig. 4*b* indicates random emission of all segments. This is the expected result for a random, extended coil. It should be pointed out, however, that we obtained diffraction-limited spots with a diameter of about 400 nm (see Fig. 1*c*), even though the completely extended chain would be over 1 $\mu$m long, what implies that these, too, must to some extent be coiled. This is in accordance with light scattering data, where the physical size of molecules in a polar solvent was only about twice that in a nonpolar solvent (18). The loose coil obviously does not allow for efficient three-dimensional energy transfer and energy migration along the chain plays an important role.

## Conclusions

Our results show that photoluminescence of conjugated polymers depends strongly on conformation. MEH-PPV in the unfavorable, nonpolar solvent toluene tends to fold in a well-organized pattern to minimize exposure to the solvent. This folding enables efficient three-dimensional energy transfer within the polymer molecule and explains the previously reported fluorescence intermittency of single polymers and their efficient quenching by electron acceptors. The observation of well-organized folding is rather surprising and reminds of the folding pattern of biomacromolecules. Conjugated polymers thus might serve as an interesting model system for the study of folding–unfolding pathways.

Polymer chains retain memory of their solution configuration even as the solvent is evaporated. Evidently, solvent evaporation is rapid compared with equilibration of the isolated chain folding geometry. This has important consequences for designing suitable processing protocols for polymer films used for electronic applications. In highly self-aggregated form, reversible jumps in intensity and polarization memory are observed because single regions of the polymer chain can dominate the photophysics.

This property is desirable for applications such as antenna complex design for energy transduction or biological sensing where attachment to an appropriate site can quench the luminescence of thousands of absorbing chromophores. Conversely, loose packing and poor energy transfer would be more desirable in fabrication of electroluminescent films where interchain interactions both reduce luminescence yield and facilitate rapid excitation transport to quench sites that form preferentially in low energy regions.

We thank Rachel Jakubiak and Yi Li (University of Rochester), X. Linda Chen, Zhenan Bao, Bell Labs, Lucent Technologies, and Fotios Papadimitrakopoulos (University of Connecticut) for the gift of samples and helpful discussions. Chris Darrow, Kelly Campos, Wigbert Siekhaus, and James J. DeYoreo (Lawrence Livermore National Library) and Wunshain Fann (National Taiwan University, Taipei) are acknowledged for stimulating discussions. This work was supported by the Laboratory Directed Research and Development Program of Lawrence Livermore National Laboratory under the auspices of the U.S. Department of Energy under Contract W-7405-ENG-48.

1. Single Molecules Special Issue (1999) *Science* **283,** 1667–1695.
2. Smith, S. B., Finzi, L. & Bustamante, C. (1992) *Science* **258,** 1122–1126.
3. Strick, T. R., Allemand, J. F., Bensimon, D., Bensimon, A. & Croquette, V. (1996) *Science* **271,** 1835–1837.
4. Florin, E. L., Moy, V. T. & Gaub, H. E. (1994) *Science* **264,** 415–417.
5. Perkins, T. T., Smith, D. E. & Chu, S. (1994) *Science* **264,** 819–822.
6. Kellermayer, M. S. Z., Smith, S. B., Granzier, H. L. & Bustamante, C. (1997) *Science* **276,** 1112–1116.
7. Ishii, Y. & Yanagida, T. (2000) *Single Molecules* **1,** 5–16.
8. Bopp, M. A., Jia, Y. W., Li, L. Q., Cogdell, R. J. & Hochstrasser, R. M. (1997) *Proc. Natl. Acad. Sci. USA* **94,** 10630–10635.
9. Dickson, R. M., Cubitt, A. B., Tsien, R. Y. & Moerner, W. E. (1997) *Nature (London)* **388,** 355–358.
10. Wu, M., Goodwin, P. M., Ambrose, W. P. & Keller, R. A. (1996) *J. Phys. Chem.* **100,** 17406–17409.
11. Bopp, M. A., Sytnik, A., Howard, T. D., Cogdell, R. J. & Hochstrasser, R. M. (1999) *Proc. Natl. Acad. Sci. USA* **96,** 11271–11276.
12. van Oijen, A. M., Ketelaars, M., Kohler, J., Aartsma, T. J. & Schmidt, J. (1999) *Science* **285,** 400–402.
13. VandenBout, D. A., Yip, W. T., Hu, D. H., Fu, D. K., Swager, T. M. & Barbara, P. F. (1997) *Science* **277,** 1074–1077.
14. Chen, L. H., McBranch, D. W., Wang, H. L., Helgeson, R., Wudl, F. & Whitten, D. G. (1999) *Proc. Natl. Acad. Sci. USA* **96,** 12287–12292.
15. Friend, R. H., Gymer, R. W., Holmes, A. B., Burroughes, J. H., Marks, R. N., Taliani, C., Bradley, D. D. C., Dos Santos, D. A., Bredas, J. L., Logdlund, M. & Salaneck, W. R. (1999) *Nature (London)* **397,** 121–128.
16. Jakubiak, R., Collison, C. J., Wan, W. C., Rothberg, L. J. & Hsieh, B. R. (1999) *J. Phys. Chem.* **103,** 2394–2398.
17. Rothberg, L. J., Yan, M., Papadimitrakopoulos, F., Galvin, M. E., Kwock, E. W. & Miller, T. M. (1996) *Synthetic Metals* **80,** 41–58.
18. Nguyen, T. Q., Doan, V. & Schwartz, B. J. (1999) *J. Chem. Phys.* **110,** 4068–4078.
19. Nguyen, T. Q., Martini, I. B., Liu, J. & Schwartz, B. J. (2000) *J. Phys. Chem.* **104,** 237–255.
20. Macklin, J. J., Trautman, J. K., Harris, T. D. & Brus, L. E. (1996) *Science* **272,** 255–258.
21. Hu, D. H., Yu, J. & Barbara, P. F. (1999) *J. Am. Chem. Soc.* **121,** 6936–6937.
22. Yan, M., Rothberg, L. J., Kwock, E. W. & Miller, T. M. (1995) *Phys. Rev. Lett.* **75,** 1992–1995.
23. Jakubiak, R., Rothberg, L. J., Wan, W. & Hsieh, B. R. (1999) *Synthetic Metals* **101,** 230–233.
24. Kersting, R., Lemmer, U., Mahrt, R. F., Leo, K., Kurz, H., Bassler, H. & Gobel, E. O. (1993) *Phys. Rev. Lett.* **70,** 3820–3823.
25. Nirmal, M., Dabbousi, B. O., Bawendi, M. G., Macklin, J. J., Trautman, J. K., Harris, T. D. & Brus, L. E. (1996) *Nature (London)* **383,** 802–804.
26. Yan, M., Rothberg, L. J., Papadimitrakopoulos, F., Galvin, M. E. & Miller, T. M. (1994) *Phys. Rev. Lett.* **73,** 744–747.